Chapter 2
Peripheral Nerve Biopsy Evaluation

Chunyu Cai

Introduction

Surgical removal of a segment of nerve leads to a permanent loss of function in that nerve and in rare cases painful injury neuromas. Therefore, a nerve biopsy is usually performed only if clinical, laboratory, and electrophysiological studies have been done, yet failed to clarify the nature or the cause of the disease. A nerve should not be biopsied if it appears normal on electrophysiological study. The major indications for nerve biopsy are clinically suspected vasculitis and amyloidosis. These disease processes are patchy; thus negative findings in a nerve biopsy does not completely exclude the above conditions. Other indications for nerve biopsy include infections (e.g. leprosy), sarcoidosis, tumor, chronic inflammatory demyelinating polyneuropathy (CIDP) that does not fully meet the electrophysiologic criteria, and hereditary neuropathies that cannot be confirmed by genetic tests [1]. In general, nerve biopsies have a higher yield in acute, multifocal, asymmetrical and severe demyelinating conditions than in chronic, symmetric and axonal types. A concomitant muscle biopsy from the same incision is advised as it may substantially increase the diagnostic yield for systemic disease processes such as vasculitis [2], amyloidosis and sarcoidosis, and causes very little additional discomfort to the patient. The muscle biopsy may also provide useful diagnostic information by confirming denervation changes in the muscle and excluding a primary myopathic process. In this chapter, we summarize biopsy procedure, specimen processing, common morphologic findings, and their diagnostic implications in peripheral nerve biopsies.

C. Cai (✉)
Department of Pathology, University of Texas Southwestern Medical Center, Dallas, TX, USA
e-mail: chunyu.cai@UTSouthwestern.edu

L. Zhou et al. (eds.), *A Case-Based Guide to Neuromuscular Pathology*,
https://doi.org/10.1007/978-3-030-25682-1_2

Nerve Biopsy Acquisition

The choice of the site and the nerve for biopsy should be made based on the clinical and electrophysiological findings. One should choose a nerve which is affected by the disease to increase the biopsy yield and to reduce the risk of neuroma formation. Distal sensory nerves such as sural nerve, superficial peroneal nerve, and superficial radial nerve are preferred as these nerves are frequently affected by inflammatory and amyloid neuropathies, and the biopsy of these nerves do not cause motor deficit. Sural nerve is the most commonly biopsied nerve. It can be biopsied alone at the lateral aspect of the distal leg with a 5-cm longitudinal incision made between the fibula and the Achille's tendon ending distally just proximal to the lateral malleolus.

Sural nerve is frequently biopsied along with gastrocnemius muscle via a single 5-cm longitudinal incision made over the midline of posterior distal leg. The biopsy is done under local anesthesia with a monitored anesthesia care. A length of 4–5 cm of nerve is biopsied. Shorter nerve biopsy specimen may hamper diagnosis yet will leave an identical sensory deficit. The risk of post-biopsy bleeding and infection is minimal. The patient may have transient irritating discomfort at the biopsy site. The sensory loss at the dorsolateral aspect of the foot usually improves with time. The neuroma formation is very rare. A combined superficial peroneal nerve and peroneus brevis muscle biopsy via a single incision may be done if the superficial peroneal nerve is more affected by the disease than the sural nerve. Superficial radial nerve biopsy is rarely done; it can be helpful when a multiple mononeuropathy only affects upper limbs. When a nerve disease (lesion) predominantly involves a proximal nerve such as sciatic nerve, median nerve at the upper arm, lumbosacral plexus, or brachial plexus, magnetic resonance neurography (MRN)-targeted fascicular nerve biopsies may be performed in a tertiary medical center by a surgeon with special expertise after communication with treating neurologist and radiologist [3].

Specimen Processing Procedure

The biopsied nerve is divided into 3 parts, a fresh specimen, a formalin fixed specimen for paraffin embedding, and a glutaldehyde fixed specimen for resin embedding, toluidine blue stain, and electron microscopy (EM). The glutaldehyde fixed specimen is superior in demonstrating myelin morphology but also most susceptible to stretching, compression and delayed fixation artifacts. The specimen must be handled with extreme care. We recommend first clamping the middle 2 cm segment of nerve in situ. Then 1 cm of nerve proximal to the clamp is excised, wrapped in a 4 × 4 gauze sponge moistened with 4 ml normal saline, and

placed in a sealed container as a fresh specimen. A 1-cm nerve fragment distal to the clamp is tied at both ends with sutures, excised and tied onto wooden tongue depressor so that the nerve is straight but not overstretched, and placed in a sealed container of 10% phosphate-buffered neutral formalin for paraffin embedding. The middle clamped segment (Fig. 2.1) is placed in a sealed container with chilled 3% glutaraldehyde for resin embedding and EM. The specimens are placed on ice for subsequent transfer from operating room to pathology laboratory, usually within 2 hours.

Once in pathology laboratory, the fresh specimen is snap frozen in isopentane cooled in liquid nitrogen. Frozen sections can be cut and stained with hematoxylin and eosin (H&E) immediately for rapid screening of vasculitis or inflammation. The formalin specimen is divided into 3–4 cross and longitudinal pieces for paraffin embedding. The glutaldehyde specimen is carefully cut out from the clamp, divided into 3 cross and 1 longitudinal pieces and further fixed in glutaldehyde overnight before epoxy resin embedding and semithin sections.

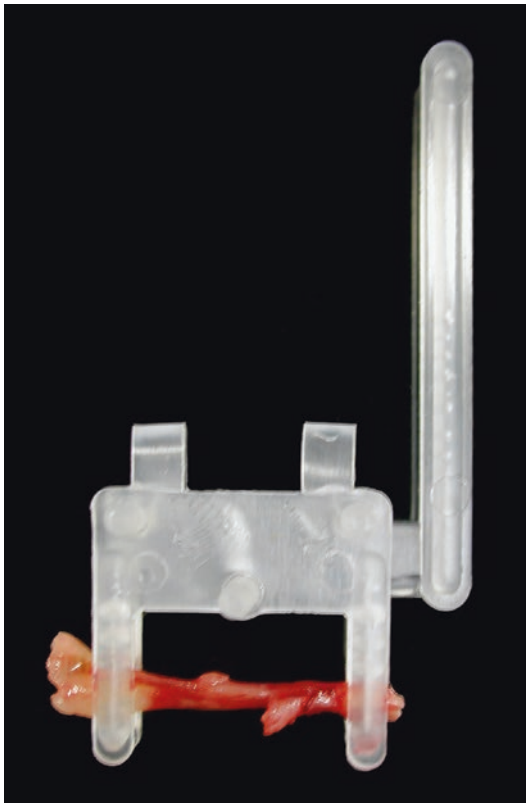

Fig. 2.1 Properly clamped peripheral nerve is fixed in glutaldehyde for resin embedding and EM processing

Routine Stains and Utilities

In our laboratory, frozen, formalin fixed and paraffin embedded (FFPE), and glutaldehyde fixed and resin embedded nerve biopsies specimens are routinely evaluated with a panel of stains as listed below.

- Frozen nerve specimen
  - H&E
  - Modified Gomori trichrome
  - Crystal violet
  - Congo red
- FFPE nerve specimen
  - H&E
  - Masson trichrome
  - Periodic acid Schiff (PAS)
  - Congo red
- Glutaldehyde fixed, resin embedded specimen
  - Toluidine blue stained thick sections for light microscopy
  - Toluidine blue stained thin sections for electron microscopy

Serial section of multiple levels on H&E stained cryostat and FFPE sections is recommended for the detection of vasculitis or inflammation. Congo red stain is performed on both cryostat and FFPE sections to increase the rate of detection for amyloidosis.

Hematoxylin and Eosin (H&E)

H&E stain provides the initial and most important morphological assessment of nerve histology, and is routinely performed on both the frozen and FFPE specimens. H&E stain is excellent in identifying vasculitis, inflammation and neoplasm, but generally offers limited value in assessing myelin or axon pathology.

One of the most important task of nerve biopsy evaluation is to identify evidence of vasculitis. The 2012 Chapel Hill Consensus Conference provides an updated classification of vasculitis [4]. Pertaining to peripheral nerve, vasculitis can be broadly dichotomized into infectious (e.g. leprosy, fungus) and noninfectious etiologies. Noninfectious vasculitis are further classified into systemic and nonsystemic vasculitic neuropathies (NSVN) [5, 6]. Morphology varies depending on the size of the vessels involved. Fibroid necrosis is more commonly seen in large ((>100 micron) to medium sized (40–100 microns) epineurial arteries [7] in polyarteritis nodosum, Churg-Strauss syndrome, Wegener's granulomatosis, ANCA associated vasculitis, or collagen vascular diseases (e.g. lupus, rheumatoid arthritis, etc.). Leukocytoclasia or perivascular lymphocytic cuffing are more commonly seen in smaller vessel (<40 microns) vasculitis such as collagen vascular disease, micro-

scopic polyangiitis [7] and NSVN [8, 9]. NSVN can only be diagnosed on a nerve biopsy and encompasses a heterogeneous and expending group of diseases such as painless diabetic radiculoplexus neuropathies, postsurgical inflammatory neuropathy, and Wartenberg migratory sensory neuropathy [5]. Subclassification of NSVN relies on clinical information and cannot be differentiated by histology alone. Takayasu arteritis, Kawasaki diseases and antiglomerular basement membrane disease do not involve peripheral nerves [5].

Acute vasculitis ***Fibrinoid necrosis with associated inflammation*** of blood vessel wall is the most definitive histological evidence of acute necrotizing vasculitis. It appears as amorphous, refractile material within arterial wall that deeply stain with eosin (Fig. 2.2a). On EM, these fibrinoid material is composed of electron dense fibrin strands with cross banding of 20.8 nm periodicity [10] (Fig. 2.2b). The origin of the fibrinoid material is believed to be polymerised fibrinogen which has permeated through the injured endothelial cell layer [11]. It should be noted that fibrinoid necrosis without inflammation can be seen in nonvasculitic conditions such as malignant hypertension [10, 12, 13] and complement mediated hypersensitivity reaction [14]. ***Transmural inflammation accompanied by karyorrhexis debris (leukocytoclasia)*** (Fig. 2.3a) carries a similar diagnostic implication as fibrinoid necrosis as definitive evidence of active vasculitis. The presence of inflammatory cells in the vessel wall or ***perivascular cuffing*** (Fig. 2.3b) of lymphocytes, while a frequent finding in vasculitis involving smaller arteries and veins, is less specific and can be seen in a variety of non-vasculitic inflammatory neuropathies including chronic inflammatory demyelinating polyneuropathy (CIDP) [15], paraneoplastic syndrome [16], as well as many other systemic inflammatory conditions. When in doubt, additional deeper levels are recommended. Presence of luminal thrombosis, endothelial damage, perivascular hemosiderin, disruption of internal elastic lamina (by elastin special stain) or separation/disruption of smooth muscle cells in media (by smooth muscle actin immunostain) support the diagnosis of vasculitis [6].

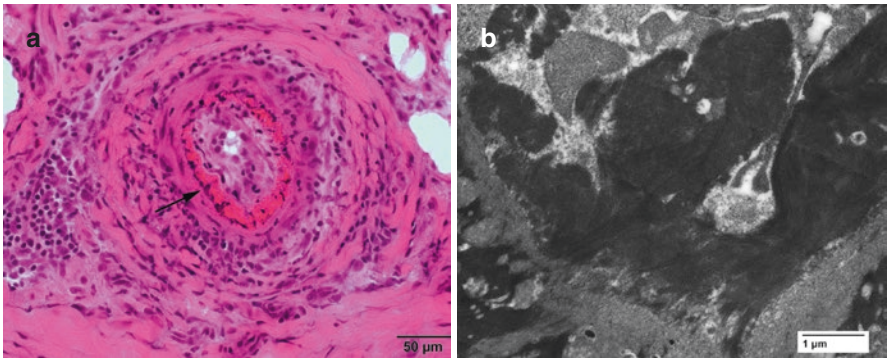

Fig. 2.2 Fibrinoid necrosis of medium sized epineurial artery. (**a**) H&E. (**b**) EM. (Images from a 78-year-old patient with rheumatoid arthritis, who presented with mononeuritis multiplex)

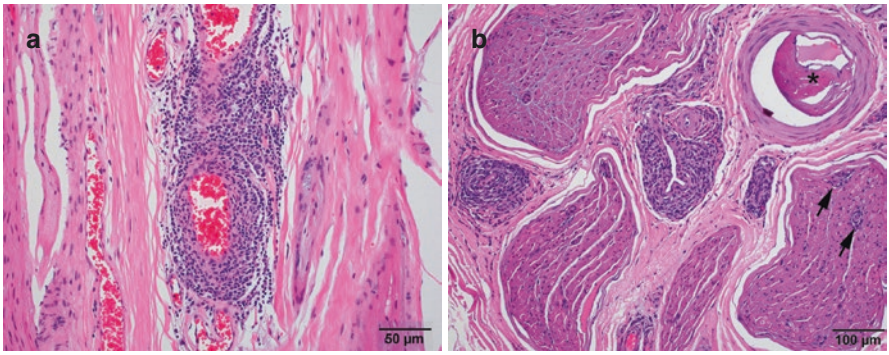

Fig. 2.3 Vessel wall inflammation. (**a**) Transmural inflammation with karyorrhexis debris is diagnostic for vasculitis. (**b**) Transmural and perivascular lymphocytic cuffing in a patient with a clinical diagnosis of diabetic amyotrophy. Panel B also shows endoneurial perivascular inflammation (arrows) and an atherosclerotic plaque within the lumen of an epineurial artery (∗)

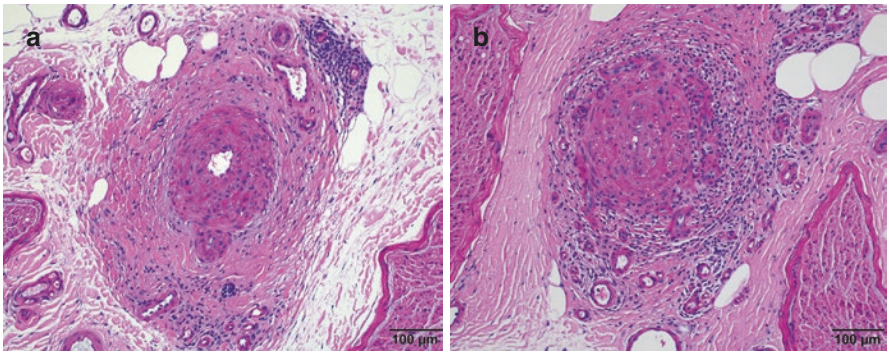

Fig. 2.4 Chronic vascular remodeling changes supportive of prior vasculitis. (**a**) PAS stain shows a medium sized epineurial artery with marked intimal and adventitia fibrosis. Two smaller vessels in the upper right corner show perivascular lymphocytic cuffing. (**b**) PAS stain of an epineurial artery with completely occluded lumen and neovascularization within and outside the lumen. (Sural nerve biopsy from a 63-year-old female with rheumatoid arthritis and progressive polyneuropathy)

Chronic vascular damage with repair Features of chronic vascular damage/repair include intimal hyperplasia, fibrosis of media, adventitia fibrosis (Fig. 2.4a), and chronic thrombosis with recanalization (Fig. 2.4b). With the presence of mononuclear inflammatory cells in the wall, these chronic vascular remodeling changes can serve as definitive evidence for vasculitis [6]. Since vasculitis is a multifocal process, additional sections or adjacent block near vessels with chronic remodeling change may demonstrate adjacent active vasculitic changes. ***Increased epineurial vessel density:*** In sural nerve, epineurial vessel number stay relatively constant throughout ages in normal person (mean 58, range 34–76), but is significantly increased in patients with vasculitic neuropathies (mean 108, range 47–179),

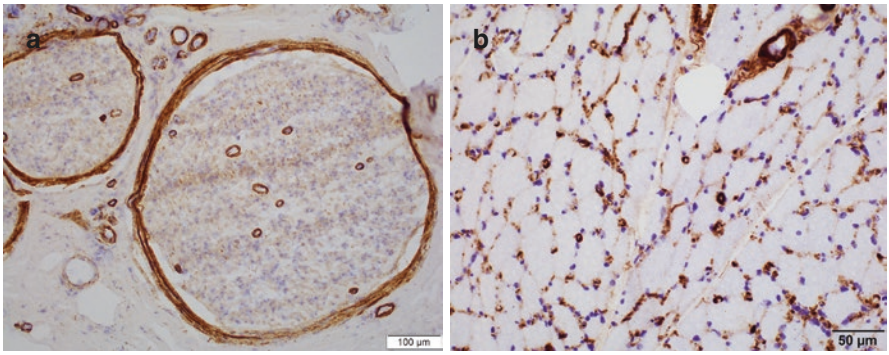

Fig. 2.5 Diffuse terminal complement complex (C5b-9) deposition in nerve (**a**) and muscle (**b**) small vessels and capillaries in a 49-year-old patient with poorly controlled diabetes

microvasculitic neuropathies (mean 110.8, range 85–131), and diabetes (Mean 106, range 85–131) [17]. The endoneurial vessel number remains remarkably constant [18]. Thus, a prominently increased number of epineurial vessels may serve as a suggestive feature for vasculitis or microvasculopathy, particularly when they are clustered or growing within the wall of vessels or perineurium (Fig. 2.4b). Increased epineurial vessels can also be seen in a significant number of nerve biopsies with mixed axonal and demyelinating features [17] and paraneoplastic syndrome [16]. Overall this is a relatively nonspecific finding that by itself conveys limited diagnostic implication. ***Arteriolosclerosis:*** Prominent thickening of the wall of endoneurial vessels is commonly associated with hypertension or diabetes. Diffuse deposition of terminal complement complex (C5b-9) in both nerve endothelial vessels and muscle capillaries is a rather characteristic feature of diabetic microangiopathy and not an indication of immune-mediated vascular injury [19] (Fig. 2.5).

Endoneurial perivascular inflammation Selective endoneurial perivascular mononuclear inflammation without significant epineurial inflammation is an uncommon finding in peripheral nerve biopsies and is a supportive feature of CIDP or Guillain-Barre syndrome (GBS) in the appropriate clinical context [16, 20]. It has also been reported in paraneopalstic syndrome [21], immune checkpoint inhibitor associated neuropathy [22], and leprosy [23]. ***Individually scattered endoneurial inflammation*** is difficult to discern on H&E. Immunostain highlighted T cells can be found in CIDP, chronic idiopathic axonal polyneuropathy, vasculitic neuropathy, as well as normal controls, thus of limited diagnostic value [24].

Perineurium pathology Inflammation that preferentially involves perineurium is associated with leprosy, which is rare in the United States but can be seen in countries with relative high incidence of leprosy, such as India, Brazil, and Indonesia [25]. Anecdotal case reports on idiopathic perineuritis [26, 27], cryoglobulinemia [28], and epidemic toxic oil syndrome [29] with preferential perineurium inflammation have been reported. Sarcoid peripheral neuropathy often shows inflammation

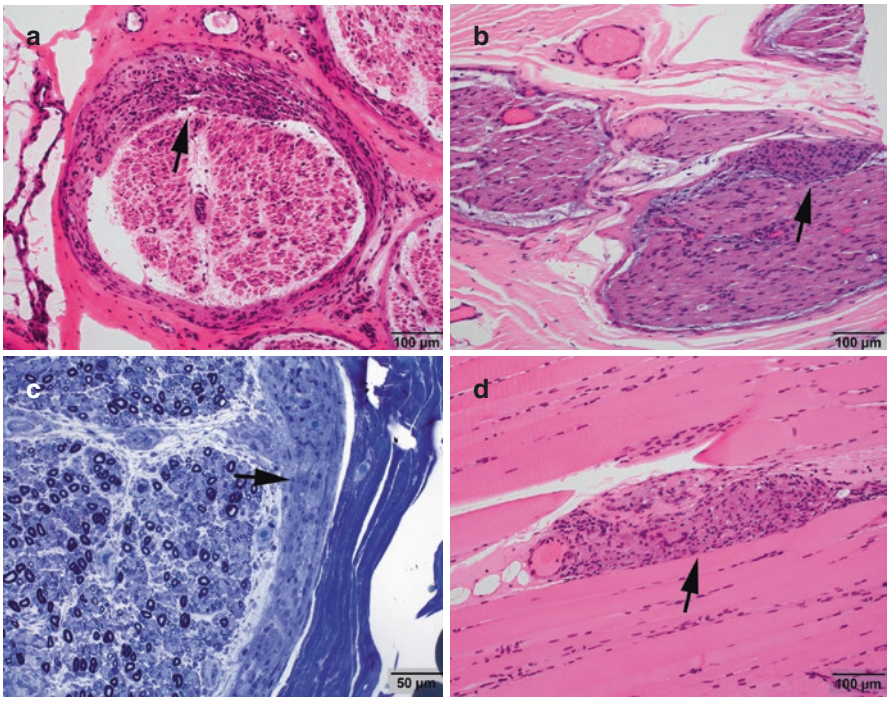

Fig. 2.6 Sarcoid perineuritis. (**a**) H&E stained cryostat section of the sural nerve shows inflammation and irregular thickening of perineurium (arrow). (**b**) Granuloma (arrow) is apparent on the paraffin fixed longitudinal nerve section. (**c**) Toluidine blue stained plastic section shows that the granulomatous inflammation (arrow) is centered on the perineurium and blood vessels. (**d**) Granulomas are also identified in the concomitant muscle biopsy. (Images from a 21-year-old patient with sarcoidosis and peripheral neuropathy)

and thickening of the perineurium [30] (Fig. 2.6). Vasculitis or other ischemic injury to the nerve fascicules can cause thickening of the perineurium, and sometimes the formation of ***injury neuroma***, characterized by the presence of microfascicles within or beyond the perineurium [31] (Fig. 2.7), even the appearance of perineuritis [32]. Injury neuromas due to trauma or prior surgery are typically larger, composed of numerous haphazardly arranged microfascicles replacing an entire fascicle or nerve. In patients with diabetic peripheral neuropathy, thickening of perineurial basal lamina and atrophy of perineurial cells (Fig. 2.8) were considered by some as a more characteristic feature of diabetic neuropathy than arteriolosclerosis [33]. ***Perineurial calcifications*** may be seen as an age related change but is more frequent and can be marked at younger age in patients with diabetic neuropathy [34] (Fig. 2.8).

Neoplasms Schwannoma, perineurioma, and neurofibroma are common peripheral nerve neoplasms that are usually excised as mass lesions and treated as general surgical pathology specimens rather than nerve biopsy. In rare occasions, lymphoma may secondarily involve a peripheral nerve and present as atypical lymphoid

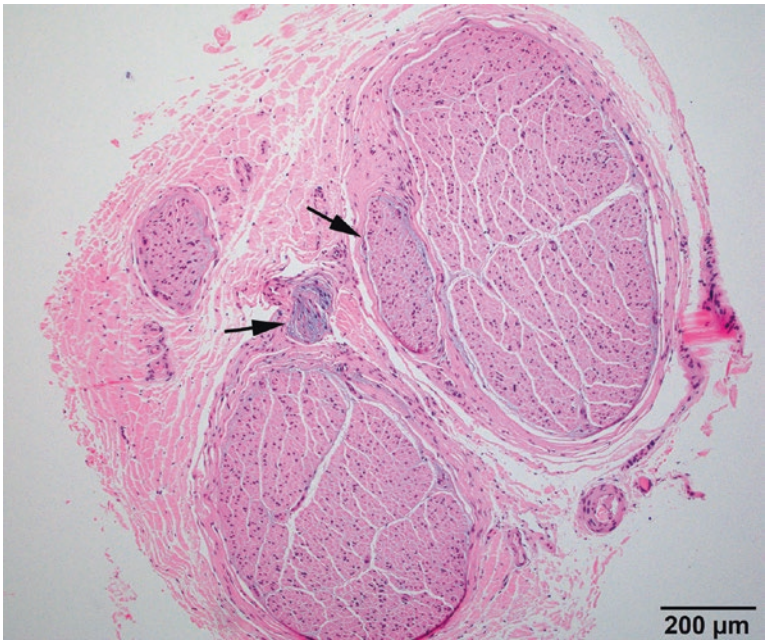

Fig. 2.7 Injury neuromas (arrows) in sural nerve biopsies are more commonly associated with prior ischemic damage rather than traumatic injury. (Image from a 57-year-old patient who presented with foot drop)

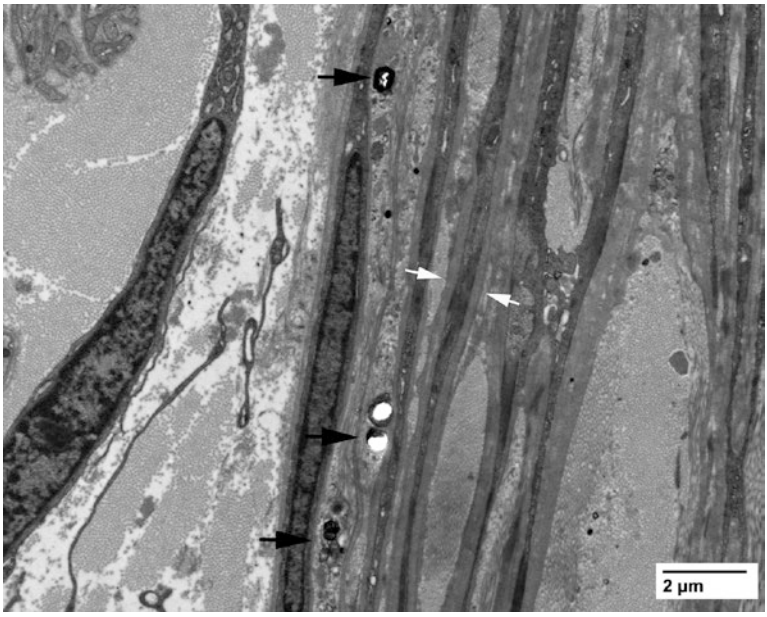

Fig. 2.8 Perineurial calcifications (black arrows) and markedly thickened basal lamina (white arrows) in a 31-year-old patient with type I diabetes

infiltrates. Intravascular B cell lymphoma can be quite subtle and the findings may be limited to small aggregates of atypical lymphoid cells within vascular lumen (Fig. 38.1). Once noticed, the diagnosis can usually be established through additional immunohistochemistry and clinical history.

Congo Red Stain

Amyloid deposits can be subtle and difficult to differentiate from hyaline on H&E stained sections (Fig. 2.9a). We routinely perform Congo red stain on both cryostat and FFPE sections of all nerve biopsies to evaluate for amyloidosis. Amyloid tends to accumulate within or around epi- or endoneurial blood vessels or in the subperineurial regions. On Congo red stained section, amyloid deposits appear orange red under regular light (Fig. 2.9b) and yellow-green birefringence under polarized light (Fig. 2.9c). A thioflavin S or T special stain is more sensitive than Congo red but requires fluorescence scope to view the amyloid deposits (Fig. 2.9d). Amyloid is also prominent on crystal violet special stain (Fig. 2.9e) and strongly accumulate terminal complement complex detectable by C5b-9 immunostain (Fig. 2.9f). On plastic section (Fig. 2.9g) and EM, the amyloid deposits are composed of haphazardly arranged fibrils. The diameter of the fibrils vary widely and range from 8–24 nanometers depending on the types of amyloid (Fig. 2.9h, i). The most common form of primary acquired amyloid neuropathy is due to immune light chain (AL) deposition that can be highlighted by Kappa or Lambda immunohistochemistry. These patients usually are over 50 years of age and have lymphoproliferative disorders, plasma cell dyscrasias or monoclonal gammopathies. Secondary amyloidosis due to infection or chronic inflammation (AA) usually does not cause polyneuropathy [35]. Patients with hereditary amyloidosis usually present early in their 30–40s but can be later. Vast majority is caused by transthyretin point mutations. The amyloid deposits are negative for immunoglobin light chains but positive on transthyretin (prealbumin) immunostain (Fig. 2.9j). Other rare forms of hereditary amyloidosis involve mutations in gesolin, apolipoprotein A1, fibrinogen A alpha chain, or lysozyme. Amyloid classification can be determined by liquid chromatography-mass spectrometry [36] followed by genetic testing.

Toluidine Blue Stained Plastic Sections

Toluidine blue stained 1.5 μm plastic section from resin embedded nerve blocks provides an accurate assessment of the number of myelinated axons and provides higher contrast and finer detail in myelin and axon morphology than frozen or FFPE specimens. Thick sections, in combination with EM when necessary, is the most important tool in determining whether the dominant pathology of a nerve is axonal degeneration, demyelination or mixed. ***Features of axonal degeneration***

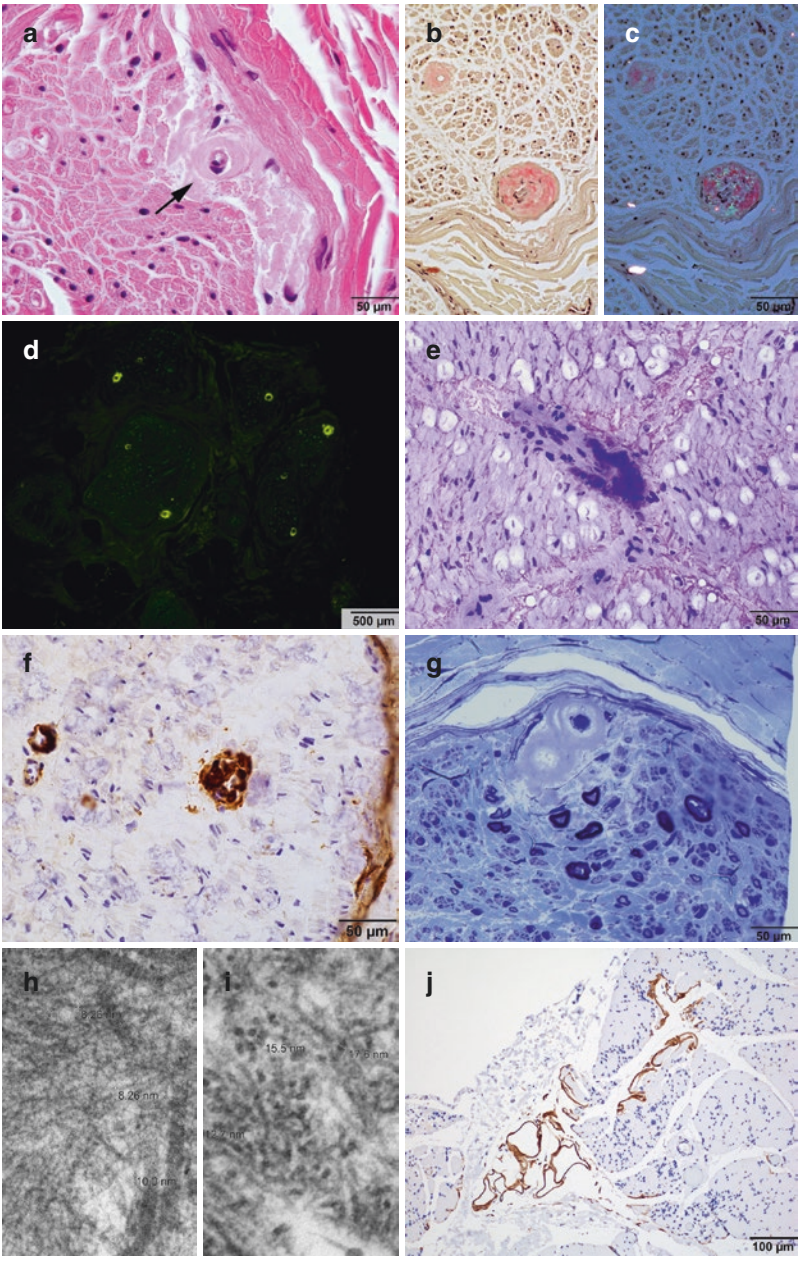

Fig. 2.9 Amyloid neuropathies. (**a**) H&E. (**b**) Congo red stain, nonpolarized light. (**c**) Congo red stain, polarized light. (**d**) Thioflavin S stain viewed under green fluorescence light. (**e**) Crystal violet stain. (**f**) C5b-9 immunostain. (**g**) Toluidine blue stained thick section. (**h**) Amyloid fibril on EM from a patient with transthyretin amyloidosis. (**i**) Amyloid fibril on EM from a patient with non-AL, non-transthyretin amyloidosis. (**j**) Transthyretin stain on the concomitant muscle biopsy from the patient with transthyretin amyloidosis

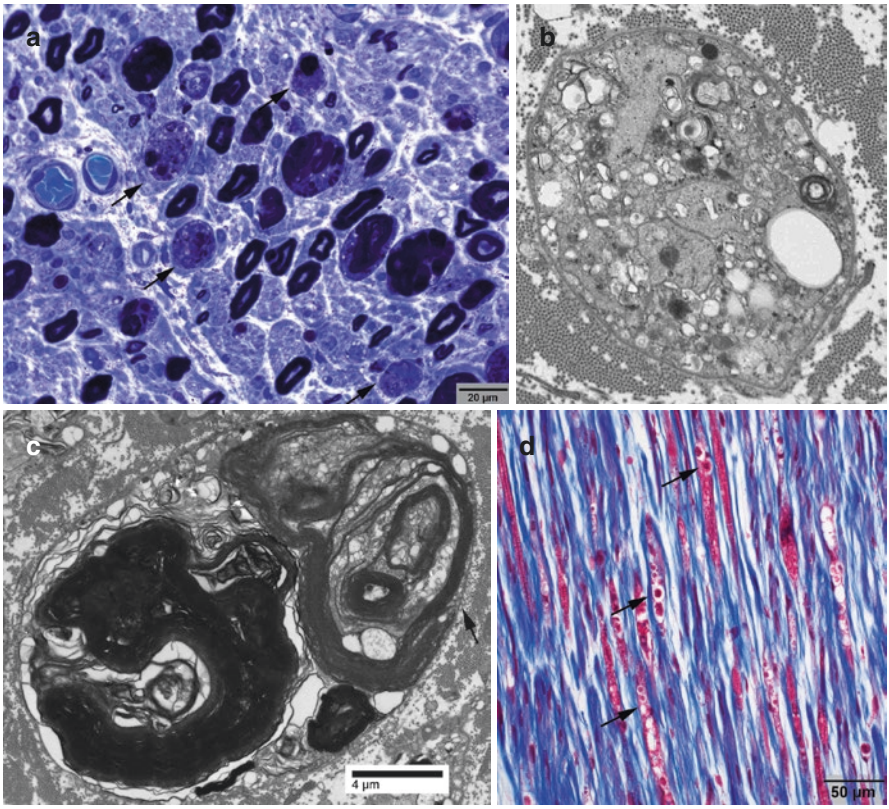

Fig. 2.10 Myeline ovoids are feature of active axonal degeneration of myelinated axons. (**a**) On toluidine blue stained thick section, myelin ovoids are round structures containing myelin debris (arrows). (**b**, **c**) On electron microscopy, myelin ovoids are composed of myelin debris at various stages of digestion still confined within the Schwann cell basal lamina (arrow) (**d**) Strings of myelin ovoids can be visualized on trichrome stained longitudinal section (arrows). (Images are from a 32-year-old patient with acute motor and sensory axonal neuropathy)

and regeneration are myelin ovoids (Fig. 2.10) and regenerating clusters (Fig. 2.11), respectively, which are readily identifiable on toluidine blue stained thick sections. They will be discussed in more detail in the EM section. ***Features of demyelination*** include naked axons, thinly myelinated axons, and segmental demyelination. Naked axons may be difficult to appreciate on light microscopy and often requires electron microscopy. Thinly myelinated axons (Fig. 2.12a, b) can be seen in regenerating clusters or regenerating axons, thus not a reliable feature of demyelination. Segmental demyelination is best appreciated on teased fiber analysis but can also be seen on longitudinally embedded toluidine stained thick sections. It should be noted though segmental demyelination is not specific for primary demyelination and can be seen in many primarily axonal processes such as diabetic neuropathy, porphyria, uremic neuropathy [37], even vasculopathies [38], these are referred to as "secondary segmental demyelination". The hallmark of ***chronic demyelination*** is the presence of true onion bulbs (Fig. 2.12c,

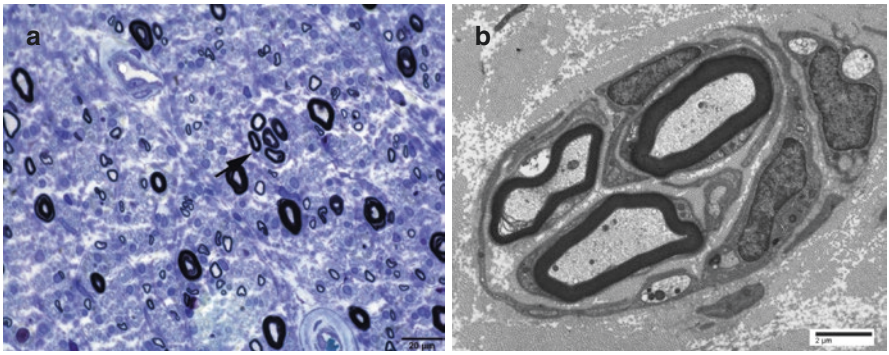

Fig. 2.11 Regenerating cluster forms in the regenerating phase following axonal degeneration, thus considered an evidence of axonopathy. (**a**) Toluidine blue. (**b**) Electron microscopy

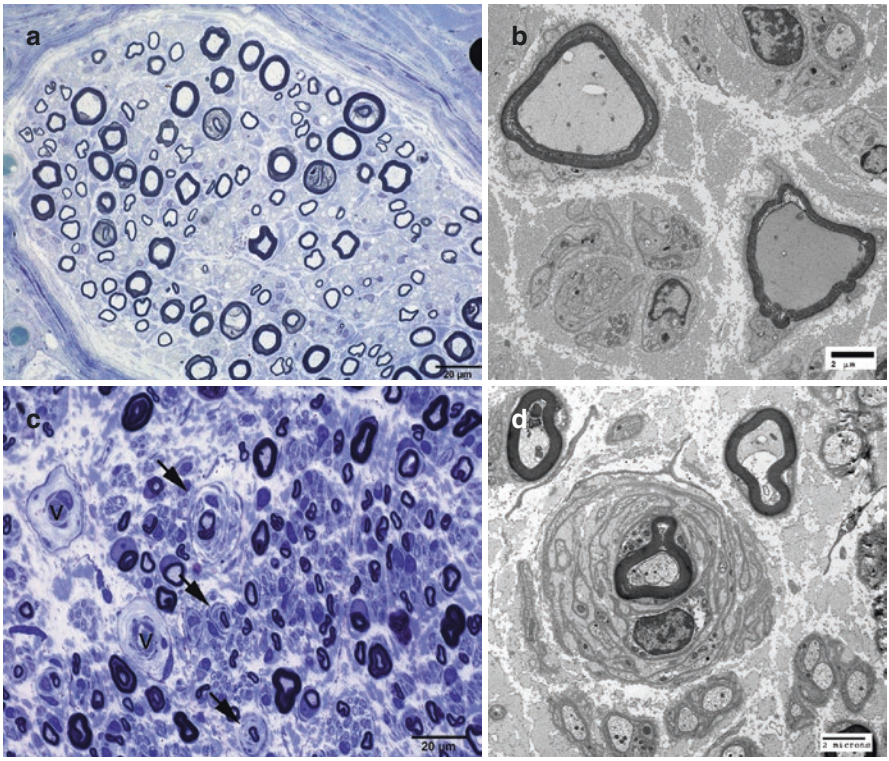

Fig. 2.12 Features of demyelination. (**a**, **b**) are images from a patient with CIDP. (**a**) Toluidine blue stained thick section show numerous thinly myelinated axons in a background without myelin ovoids or regenerating clusters. (**b**) EM shows that the axons are intact and not associated with regenerating clusters. (**c**, **d**) are images from a separate patient with CIDP. (**c**) Toluidine blue stained thick section shows multiple well-formed onion bulbs (arrows). "v" indicate vessels.(**d**) EM shows that the onion bulbs are composed of a central thinly myelinated axon surrounded by multiple layers of supernumerary Schwann cell processes. No other myelinated or unmyelinated axons are present within the onion bulb to suggest a regenerating cluster

d), which results from repeated cycles of demyelination and re-myelination that leads to the buildup of multiple concentric layers of Schwann cell processes and their basal lamina. In practice, determination of primary axonal degeneration versus demyelination often relies on the dominant pathology of the nerve, e.g. occasional thinly myelinated fibers in a background of frequent myelin ovoids and regenerating clusters are likely axonal, while abundant thinly myelinated axons or onion bulbs with minimal associated axonal degeneration supports primary demyelination. When comparable amount of axonal and myelin alterations are present, a descriptive "mixed axonal and demyelinating features" is rendered. This is a nonspecific but relatively common finding in patients with diabetic peripheral neuropathy.

Differential fascicular loss of myelinated axons (Fig. 2.13) is commonly considered an indirect evidence of vasculitic neuropathy. However, it can be seen in CIDP (also referred to as "multifocal loss" of myelinated fibers [16]) and chronic nerve compression [39]. ***Subperineurial edema*** is an abnormal finding in sural nerve readily detectable on H&E but best viewed on toluidine blue stained plastic sections (Fig. 2.13). It is generally considered an indicator for inflammatory neuropathies such as vasculitis, CIDP and GBS. The degree of edema is more prominent in inflammatory neuropathies with recent onset [40]

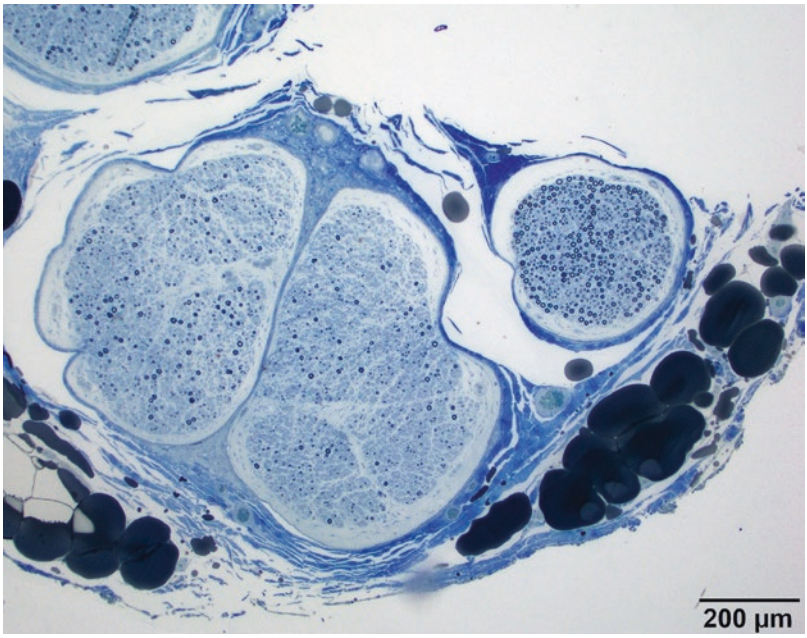

Fig. 2.13 Differential fascicular loss of axons. Toluidine blue section shows severe depletion of axons in the left two fascicles but well preserved axons in the fascicle on the top right. All fascicle show prominent subperineurial edema. (Sural nerve biopsy from a 17-year-old patient with axonal neuropathy)

but has no correlation with the severity of axon loss. However, subperineurial edema is nonspecific and has been well documented in many non-inflammatory conditions such amyloidosis [41], lead poisoning [42], thiamine deficiency [43], immune checkpoint inhibitor chemo reagents [22], chronic nerve compression [39], as a non-exhaustive list.

Electron Microscopy (EM)

While thick section viewed at the light microscopy resolution can provide a general assessment of large myelinated axon density, myelin thickness, and the presence of ovoids, regenerating clusters, and well-formed onion bulbs, many important diagnostic features can only be assessed by EM, such as macrophage mediated demyelination, presence of naked axons or early degenerating axons, true onion bulb versus pseudo-onion bulb, and integrity and density of unmyelinated axons. We perform electron microscopy on most of nerve biopsies when an etiologic diagnosis (e.g. vasculitis, amyloidsis) is not apparent on routine histological sections. In each case multiple 1.5 μm thick sections from a total of four resin embedded nerve blocks are first reviewed by light microscopy. The most representative block is selected, from which 100 nanometer thin sections are cut, mounted on a copper grid, stained, and viewed by electron microscopy.

Features of axonal degeneration and regeneration When an axon is injured, most often by trauma or ischemia, the axon and its myelin sheath distal to the injury site undergo a sequence of events referred to as ***Wallerian degeneration***. The neuron is still viable which will then attempt to regenerate the axon from the proximal stump, forming regenerating cluster. The very first sign of axonal degeneration is i***ncreased organelles*** (mainly mitochondria) due to cessation of axonal transport, occurring within 12–24 hours of axon injury (Fig. 2.14a). This is followed by degeneration of the axoplasm with loss of structure, rarification, and eventually disappearance of the axon (Fig. 2.14b, c). The myelin sheath subsequently collapses and degenerates, forming ***myelin ovoids*** (Fig. 2.14d). The initial phase of myelin degeneration occurs in the Schwann cell cytoplasm, the remnants are then removed by macrophages (Fig. 2.14e). The macrophages can be distinguished from Schwann cells by their filopodia (arrows) and the lack of a basement membrane. The Schwann cell unit devoid of myelinated axon collapses (Fig. 2.14f). Regeneration occurs at the viable tip of the proximal stump, where a growth cone is formed and extends multiple axon sprouts. Meanwhile, Schwann cells proliferate within the original basement membrane tube and guide axon growth, forming ***Bands of Büngner*** (Fig. 2.14g). The ***regenerating cluster*** follows when individual axon sprout becomes associated with a Schwann cell which produces its own basement membrane and myelin. The original basement membrane tube is usually degenerated by this time (Fig. 2.14h). The axon sprouts that do not reach a target will disappear, while usually one dominant regenerating axon will remain. The myelin sheath of the regenerating axon is thin-

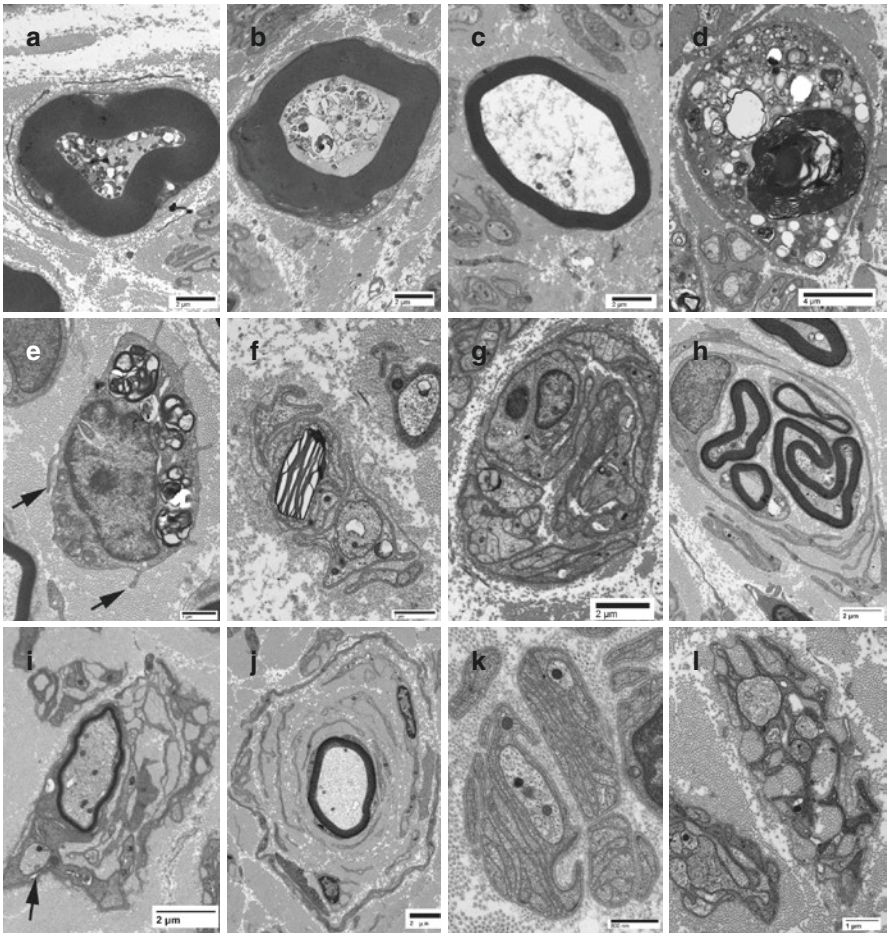

Fig. 2.14 Features of axonal degeneration/regeneration on EM. (**a**) Early degenerating axon with increased organelle. (**b**, **c**) Mid to late degenerating axons with degeneration and dissolution of axoplasm. (**d**) Myelin ovoid. (**e**) Macrophage containing myelin debris. Arrows indicate filopodia. (**f**) Collapsed Schwann cell unit devoid of axon. The presence of Reich granule at the center indicates this was a myelinating Schwann cell with an axon. (**g**) Bands of Bungner. (**h**) Regenerating cluster (**i**) Pseudo-onion bulb contain unmyelinated axons (arrow) within the Schwann cell processes and is a feature of axonopathy. (**j**) True onion bulb does not contain unmyelinated axons and is a feature of chronic demyelination. (**k**) Stacked Schwann cell processes and (**l**) Clustered collagen pockets indicate loss of unmyelinated axons

ner than normal axons of similar caliber and gives the appearance of a ***Pseudo-onion bulb,*** a central thinly myelinated axon surrounded by proliferating, sometimes concentric Schwann cell processes (Fig. 2.14i). Pseudo-onion bulbs are thus considered a feature of axonopathy rather than demyelination. The presence of unmyelinated axons within the Schwann cell processes differentiate pseudo-onion bulbs (Fig. 2.14i arrow) from a true onion bulb (Fig. 2.14j). ***Stacked Schwann cell pro-***

cesses is a feature of degeneration of unmyelinated axons (Fig. 2.14k). The flatness of Schwann processes and the lack of a common basal lamina tube differ from bands of Büngner. Occasional ***collagen pockets*** can be seen in normal sural nerve but clustered collagen pockets indicate unmyelinated axonal loss (Fig. 2.14l).

Features of demyelination ***Macrophage mediated demyelination***, characterized by macrophage entering Schwann cell basement membrane and directly contacting or stripping the myelin sheath off an intact axon (Fig. 2.15a), is considered a definitive diagnostic feature of active immune mediated demyelination (e.g. GBS or CIDP). Macrophage mediate demyelination is rarely seen in peripheral nerve biopsies, however, as axons do not stay demyelinated for long in CIDP, and peripheral nerve biopsy is rarely done in the acute phase of GBS. The diagnosis of CIDP on a nerve biopsy often relies more on the presence of prominent endoneurial lymphohistiocytic inflammation, and evidence of demyelination of intact associated axons. Individual axon devoid of myelin sheath (also referred to as "***naked axons***") comparable in size to adjacent myelinated axons is a feature of demyelination (Fig. 2.15b). Care should be taken not to confuse naked axons with nodes of Ranvier, which are the gap areas between two adjacent myelinating Schwann cells where the axon is not covered by myelin sheath. Node of Ranvier is a normal structure, not evidence of demyelination, and can be differentiated from a naked axon by the presence of nodal processes (Fig. 2.15c). ***Onion bulb*** is a feature of chronic demyelination and has been discussed in the section above. ***Vesicular degeneration of myelin*** in a well preserved nerve biopsy specimen is considered evidence of demyelination. However, in most situations encountered in nerve biopsy, it is more likely a result of delayed fixation artifact (Fig. 2.15d). Widely spaced myelin and uncompacted myelin are rare myelin abnormalities but have important diagnostic implications when detected. ***Widely spaced myelin (WSM)*** refers to increased space between myelin laminae (Fig. 2.15e). Majority of WSM cases are associated with Waldenstrom's macroglobulinemia with circulating IgM paraprotein against myelin associated glycoprotein (anti-MAG) activity [44]. A minority of cases have been reported in association with IgM monoclonal gammopathy of undetermined significance and anti-MAG activity. ***Uncompacted myelin*** refers to separation of the major dense lines of myelin (Fig. 2.15f) and is most frequently reported in association with POEMS syndrome [45]. It has also been reported in dysglobulinemic neuropathies [46], Waldenström's macroglobulinemia [44], monoclonal gammopathies [47], and a range of hereditary neuropathies with mutations in myelin associated proteins [48, 49].

Other Miscellaneous ***EM findings and artifacts*** ***Polyglucosan bodies*** are round, laminated intra-axonal inclusions that are morphologically identical to corpora amylacea and Lafora bodies (Fig. 2.16a). They are strongly PAS positive and diastase resistant (Fig. 2.16b, c). On EM, polyglucosan bodies are composed mostly of filamentous polysaccharide (Fig. 2.16d–f). While frequent polyglucosan bodies in multiple nerve fascicles are diagnostic for adult polyglucosan disease in the case featured by the Fig. 2.16, the finding of isolated polyglucosan

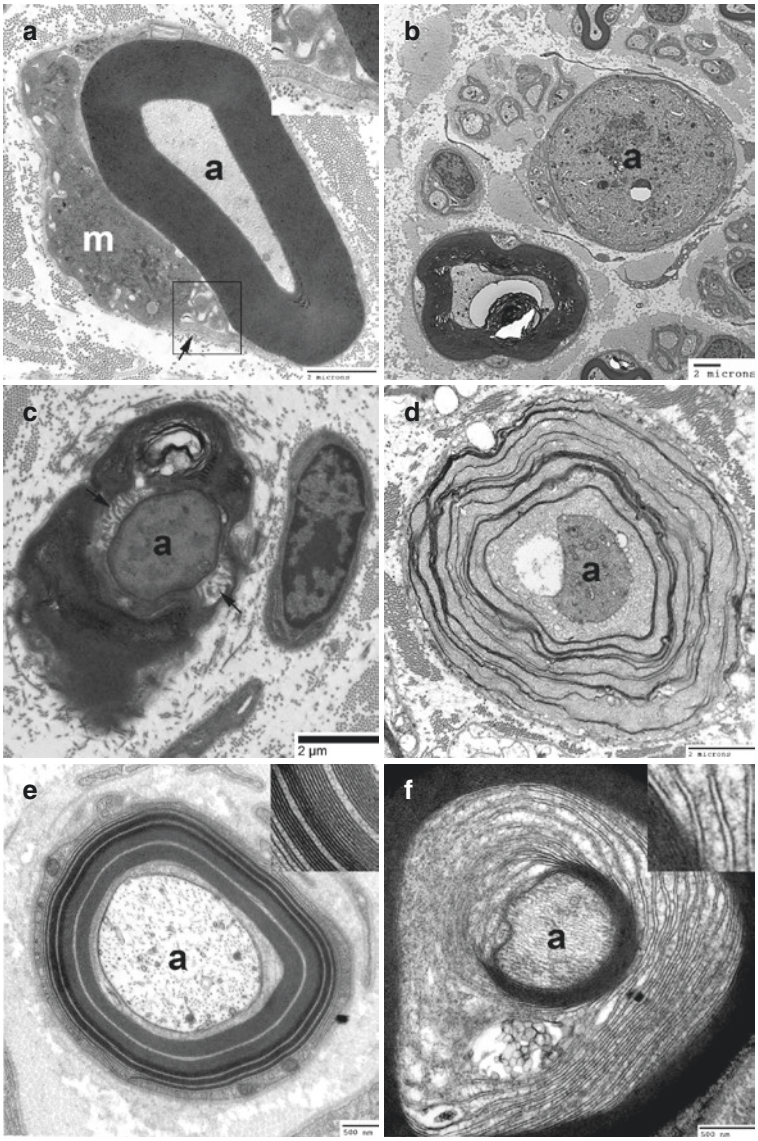

Fig. 2.15 Features of demyelination on EM. (**a**) Macrophage mediated demyelination. A macrophage (m) is within the basement membrane (arrow) of a Schwann cell containing a myelinated axon (a). The macrophage filopodia are in direct contact of the myelin sheath (inset) (Image from a 74-year-old man with fulminant GBS). (**b**) Naked axon (a) in a patient with CIDP. (**c**) Not all large unmyelinated axon profile represents demyelination. Axon segment at the node of Ranvier is unmyelinated. The presence of nodal processes (arrows) distinguishes node of Ranvier from naked axons. (**d**) Vesicular myelin degeneration due to delayed fixation artifact in an infant autopsy nerve. (**e**) Widely spaced myelin is associated with Waldenstrom Macroglobulinemia with anti-MAG IgM and characterized by increased space between myelin laminae (inset). (**f**) Uncompacted myelin is associated with POEMS syndrome and characterized by separation of the major dense line (inset). (Image panels **a**, **d**, **e**, and **f** are provided by Dr. Robert E. Schmidt, Department of Pathology and Immunology, Washington University School of Medicine at St. Louis, MO)

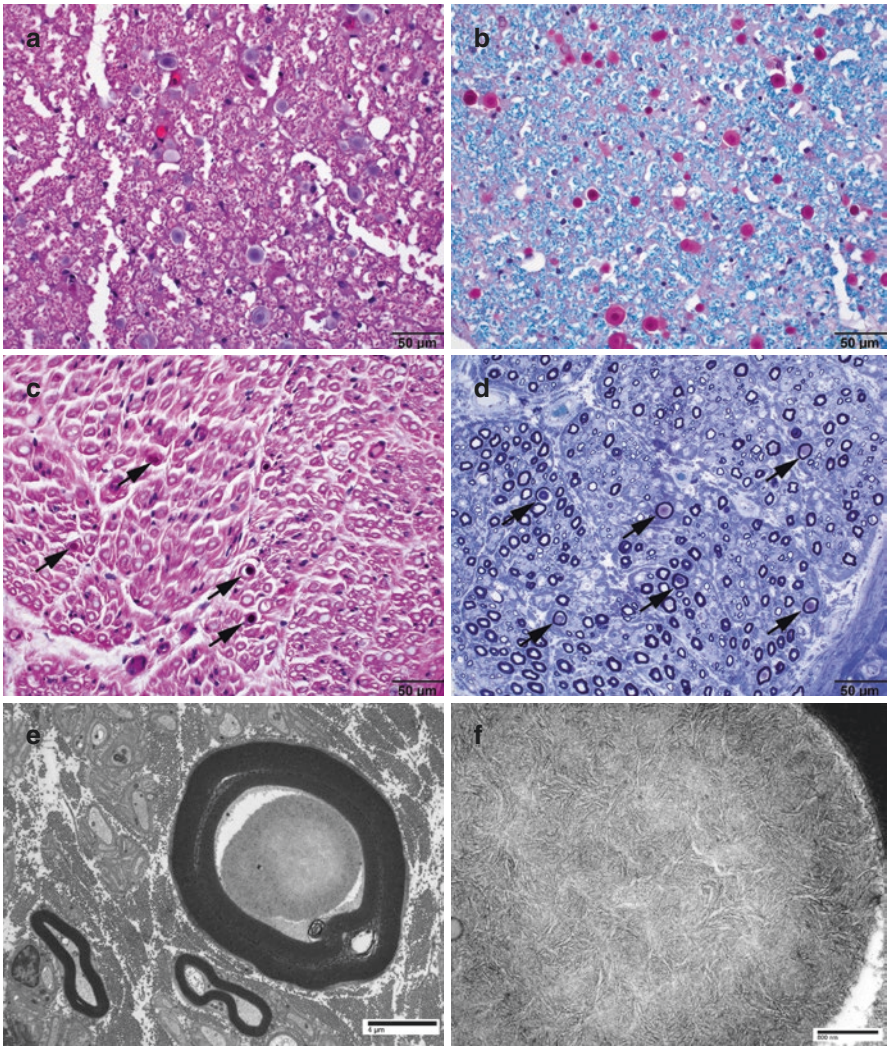

Fig. 2.16 Images of polyglucosan bodies from an autopsy patient who died from adult polyglucosan disease at age 49 years. H&E (**a**) and Luxol-fast blue/PAS stains (**b**) show numerous polyglucosan bodies throughout the central nervous system (Images A&B are from the dorsal column of spinal cord). PAS stain (**c**) and toluidine blue stained thick sections of the peroneal nerve (**d**) show multiple intra-axonal polyglucosan bodies. On electron microscopy (**e**, **f**), the polyglucosan bodies are mainly composed of filamentous polysaccharide

body is less specific and can also be seen as a common age related nonspecific change in normal person [50]. ***Renaut bodies*** are whorled structures located in the subperineurial regions (Fig. 2.17a, b). On EM they are composed of collagen, intermediate filaments, and fibroblast processes (Fig. 2.17c). Renaut body can be seen in normal person as an age related change [51]. Frequent Renaut bodies are associated with chronic nerve impingement [52] and may provide

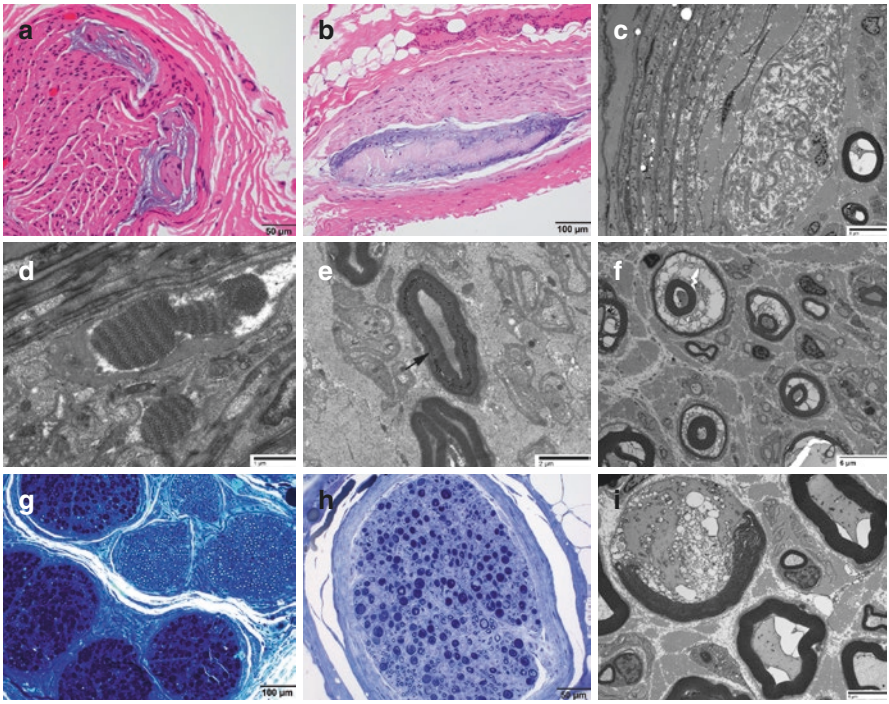

Fig. 2.17 Miscellaneous findings and artifacts. (**a**–**c**) Renaut bodies on H&E stained cross section (**a**), longitudinal section (**b**) and EM (**c**). (**d**) Luse body (fibrous long spacing collagen) on EM. (**e**) Schmidt-Lanterman incisure (arrow). (**f**) In poorly preserved specimen, the Schmidt-Lanterman spaces are often markedly enlarged. (**g**–**i**): compression artifacts due to rough handling. (**g**) Toluidine blue stained thick section shows compression artifacts of the four fascicles on the left. (**h**) Large myelinated axons are most susceptible to compression artifacts. Smaller myelinated axons are better preserved. (**i**) Artifactually damaged myelin may retract from the axon and create half myelin

diagnostic value in peripheral nerves resected due to chronic neurogenic pain. ***Luse bodies*** are fusiform structures composed of fibrous long-spacing collagen that resemble raccoon tail on EM (Fig. 2.17d). Luse bodies are originally described by Luse in Schwannomas [53]. In sural nerve biopsies, they are typically found in the perineurium or endoneurium and represent a nonspecific finding that carries no diagnostic implications. They can be seen in normal nerves [54, 55] and a range of neoplastic and non-neoplastic conditions. ***Schmidt-Lanterman incisures*** are cleft like space of noncompaction that is normally present within the myelin sheath (Fig. 2.17e). In poorly preserved or fixed nerve specimens, the Schmidt-Lanterman incisures are often enlarged and may contain disrupted or vesicular myelin (Fig. 2.17f). ***Reich Pi granules.*** Small Pi granules are a normal component of Schwann cells associated with myelinated axons. In Schwann cell units devoid of axons, the presence of large Pi granules indicates

loss of myelinated axons (Fig. 2.14f). ***Crush artifacts:*** The myelin sheath is composed of semi-liquid lipid-protein bilayers with no mechanic strength, and thus highly subject to prefixation manipulation damages. A common compression artifact is "blue blobs", which may selectively affect some fascicles of a nerve (Fig. 2.17g) or a subset of fibers within a fascicle (Fig. 2.17h). Large myelinated axons are most susceptible to compression damage. On EM, the broken myelin sheath may retract and create a half ring around the axon (Fig. 2.17i), which should not be mistaken with myelinopathy.

Teased Fiber Analysis

Teased fiber analysis is the preferred method in differentiating primary from secondary segmental demyelination, and is more sensitive in detecting tomacula. However, fiber teasing is quite laborious and a sufficient number of cases is required for performers to maintain technical skill and proficiency. Many centers consider nerve fiber teasing to be insufficiently informative to justify its cost in routine evaluation of sural nerve biopsies [1]. In one study, teased fiber analysis added critical information to other classical techniques in only 4/102 cases [56]. At our institution, we have essentially stopped requesting teased fiber analysis for routine nerve biopsy evaluation.

Special Stains and Utilities

A variety of special stains can be utilized to highlight certain structures in peripheral nerve biopsy. ***Gomori's trichrome*** stain is performed on cryostat section of peripheral nerve and stains myelin red and collagen blue, thus may provide a quick assessment of the density and distribution of myelinated axons (Fig. 2.18). ***Masson's trichrome*** similarly stains myelin red on formalin fixed nerve segment and can well demonstrate myelin ovoids on longitudinal sections (Fig. 2.10d). ***Periodic acid Schiff (PAS)*** stains basement membrane in blood vessels and perineurium (Fig. 2.4), and also intensely stain polyglucosan bodies (Fig. 2.16c). ***Elastin (Verhoeff-van Gieson, or VVG)*** stain highlights internal elastic lamina of arteries in case where chronic vascular damage is suspected. ***Crystal violet*** stain can help highlight amyloid and metachromatic deposits in metachromatic leukodystrophy. ***Modified Grocott's methenamine silver (GMS)*** and ***acid fast bacillus (AFB)*** stains are occasionally performed when granulomatous inflammation is present to exclude fungal or mycobacteria organisms. ***Fite*** stain helps demonstrate mycobacterium leprae and other weakly acid fast bacteria.

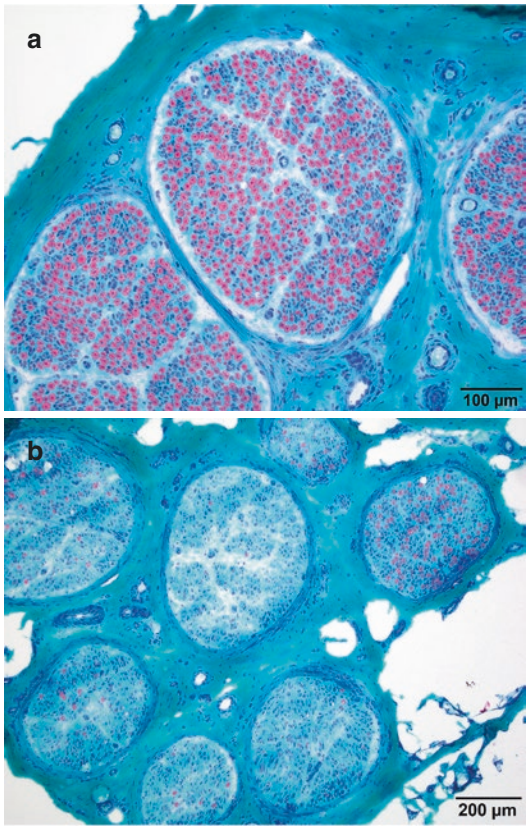

Fig. 2.18 Gomori trichrome stain highlights nerve myelin sheath in red. (**a**) Normal nerve. (**b**) A nerve with prominent differential fascicular loss of myelinated axons suggestive of a vascular etiology

Immunostains

Standard immunohistochemical (IHC) stains can be performed on FFPE never tissue to characterize inflammatory infiltrates, to highlight individual nerve or vascular components, and to classify neoplastic cells. Here we describe some commonly utilized IHCs and there utilities. ***CD45*** (leukocyte common antigen) stains all white blood cells and is commonly used to highlight any inflammatory cells. ***CD3*** is a common T cell marker that stains both helper T cells (***CD4*** positive) and cytotoxic T cells (***CD8*** positive). ***CD20*** is a B cell marker. ***CD68*** stains macrophages. ***CD31*** and ***CD34*** are an endothelial cell markers that help highlight blood vessels. ***Smooth muscle antigen (SMA)*** stains smooth muscle cells and helps to highlight vessel wall alterations in vasculitis cases. Regarding nerve components, ***neurofilament protein (NFP)*** and ***PGP9.5*** stains axons. ***Neural cell adhesion molecule (NCAM)*** is a marker for non-myelinating Schwann cells that highlights Remak bundles (unmyelinated fibers). ***Myelin basic protein*** and $\boldsymbol{P_0}$ stain myelin sheath. ***S100*** is a more general Schwann cell marker but is usually used in the context of neoplasms (i.e. Schwannoma, neurofibroma) rather than non-neoplastic nerve biopsies. ***Epithelial***

membrane antigen (EMA) stains perineurium. Finally, when amyloid is found, ***transthyretin, kappa,*** and ***lambda*** light chain immunostains can help further classify some cases into hereditary and acquired amyloidosis subtypes.

References

1. Sommer C, Brandner S, Dyck PJ, Magy L, Mellgren SI, Morbin M, et al. 147th ENMC international workshop: guideline on processing and evaluation of sural nerve biopsies, 15–17 December 2006, Naarden, The Netherlands. Neuromuscul Disord NMD. 2008;18(1):90–6.
2. Vital C, Vital A, Canron MH, Jaffre A, Viallard JF, Ragnaud JM, et al. Combined nerve and muscle biopsy in the diagnosis of vasculitic neuropathy. A 16-year retrospective study of 202 cases. J Peripher Nerv Syst JPNS. 2006;11(1):20–9.
3. Dyck PJ, Dyck PJB, Klein CJ, Low P, Amrami K, Engelstad J, et al. Companion to peripheral neuropathy E-book: illustrated cases and new developments: Elsevier Health Sciences; Philadelphia, PA. 2010. p. 3–23.
4. Jennette JC, Falk RJ, Bacon PA, Basu N, Cid MC, Ferrario F, et al. 2012 revised international Chapel Hill consensus conference nomenclature of vasculitides. Arthritis Rheum. 2013;65(1):1–11.
5. Collins MP, Hadden RD. The nonsystemic vasculitic neuropathies. Nat Rev Neurol. 2017;13(5):302–16.
6. Collins MP, Dyck PJ, Gronseth GS, Guillevin L, Hadden RD, Heuss D, et al. Peripheral nerve society guideline on the classification, diagnosis, investigation, and immunosuppressive therapy of non-systemic vasculitic neuropathy: executive summary. J Peripher Nerv Syst JPNS. 2010;15(3):176–84.
7. Ohkoshi N, Mizusawa H, Oguni E, Shoji S. Sural nerve biopsy in vasculitic neuropathies: morphometric analysis of the caliber of involved vessels. J Med. 1996;27(3–4):153–70.
8. Sugiura M, Koike H, Iijima M, Mori K, Hattori N, Katsuno M, et al. Clinicopathologic features of nonsystemic vasculitic neuropathy and microscopic polyangiitis-associated neuropathy: a comparative study. J Neurol Sci. 2006;241(1–2):31–7.
9. Dyck PJ, Benstead TJ, Conn DL, Stevens JC, Windebank AJ, Low PA. Nonsystemic vasculitic neuropathy. Brain J Neurol. 1987;110(Pt 4):843–53.
10. Heath D, Smith P. The electron microscopy of "fibrinoid necrosis" in pulmonary arteries. Thorax. 1978;33(5):579–95.
11. Amano S. Vascular changes in the brain of spontaneously hypertensive rats: hyaline and fibrinoid degeneration. J Pathol. 1977;121(2):119–28.
12. Pitcock JA, Johnson JG, Hatch FE, Acchiardo S, Muirhead EE, Brown PS. Malignant hypertension in blacks. Malignant intrarenal arterial disease as observed by light and electron microscopy. Hum Pathol. 1976;7(3):333–46.
13. Rosenblum WI. Fibrinoid necrosis of small brain arteries and arterioles and miliary aneurysms as causes of hypertensive hemorrhage: a critical reappraisal. Acta Neuropathol. 2008;116(4):361–9.
14. Renkawek K, Majkowska-Wierzbicka J, Krajewski S. Necrotic changes of the spinal cord with immune-complex-mediated disseminated vasculitis in a case of atypical allergic encephalomyelitis. J Neurol. 1985;232(6):368–73.
15. Rizzuto N, Morbin M, Cavallaro T, Ferrari S, Fallahi M, Galiazzo Rizzuto S. Focal lesions area feature of chronic inflammatory demyelinating polyneuropathy (CIDP). Acta Neuropathol. 1998;96(6):603–9.
16. Piccione EA, Engelstad J, Dyck PJ, Mauermann ML, Dispenzieri A, Dyck PJ. Nerve pathologic features differentiate POEMS syndrome from CIDP. Acta Neuropathol Commun. 2016;4(1):116.

17. Schutz G, Schroder JM. Number and size of epineurial blood vessels in normal and diseased human sural nerves. Cell Tissue Res. 1997;290(1):31–7.
18. Mawrin C, Schutz G, Schroder JM. Correlation between the number of epineurial and endoneurial blood vessels in diseased human sural nerves. Acta Neuropathol. 2001;102(4):364–72.
19. Yell PC, Burns DK, Dittmar EG, White CL 3rd, Cai C. Diffuse microvascular C5b-9 deposition is a common feature in muscle and nerve biopsies from diabetic patients. Acta Neuropathol Commun. 2018;6(1):11.
20. Ubogu EE. Inflammatory neuropathies: pathology, molecular markers and targets for specific therapeutic intervention. Acta Neuropathol. 2015;130(4):445–68.
21. Vallat JM, Leboutet MJ, Hugon J, Loubet A, Lubeau M, Fressinaud C. Acute pure sensory paraneoplastic neuropathy with perivascular endoneurial inflammation: ultrastructural study of capillary walls. Neurology. 1986;36(10):1395–9.
22. Manousakis G, Koch J, Sommerville RB, El-Dokla A, Harms MB, Al-Lozi MT, et al. Multifocal radiculoneuropathy during ipilimumab treatment of melanoma. Muscle Nerve. 2013;48(3):440–4.
23. Chimelli L, Freitas M, Nascimento O. Value of nerve biopsy in the diagnosis and follow-up of leprosy: the role of vascular lesions and usefulness of nerve studies in the detection of persistent bacilli. J Neurol. 1997;244(5):318–23.
24. Bosboom WM, Van den Berg LH, De Boer L, Van Son MJ, Veldman H, Franssen H, et al. The diagnostic value of sural nerve T cells in chronic inflammatory demyelinating polyneuropathy. Neurology. 1999;53(4):837–45.
25. Global leprosy update, 2016: accelerating reduction of disease burden. Releve epidemiologique hebdomadaire. 2017;92(35):501–19.
26. Bourque CN, Anderson BA, Martin del Campo C, Sima AA. Sensorimotor perineuritis--an autoimmune disease? Can J Neurol Sci. 1985;12(2):129–33.
27. Simmons Z, Albers JW, Sima AA. Case-of-the-month: perineuritis presenting as mononeuritis multiplex. Muscle Nerve. 1992;15(5):630–5.
28. Konishi T, Saida K, Ohnishi A, Nishitani H. Perineuritis in mononeuritis multiplex with cryoglobulinemia. Muscle Nerve. 1982;5(2):173–7.
29. Ricoy JR, Cabello A, Rodriguez J, Tellez I. Neuropathological studies on the toxic syndrome related to adulterated rapeseed oil in Spain. Brain J Neurol. 1983;106 (. Pt 4:817–35.
30. Said G, Lacroix C, Plante-Bordeneuve V, Le Page L, Pico F, Presles O, et al. Nerve granulomas and vasculitis in sarcoid peripheral neuropathy: a clinicopathological study of 11 patients. Brain J Neurol. 2002;125(Pt 2):264–75.
31. Dyck PJ, Engelstad J, Norell J, Dyck PJ. Microvasculitis in non-diabetic lumbosacral radiculoplexus neuropathy (LSRPN): similarity to the diabetic variety (DLSRPN). J Neuropathol Exp Neurol. 2000;59(6):525–38.
32. Lee SS, Yoon TY. Sensory perineuritis presented as a mononeuritis multiplex associated with livedo vasculitis. Clin Neurol Neurosurg. 2001;103(1):56–8.
33. Bradley JL, Thomas PK, King RH, Watkins PJ. A comparison of perineurial and vascular basal laminal changes in diabetic neuropathy. Acta Neuropathol. 1994;88(5):426–32.
34. King RH, Llewelyn JG, Thomas PK, Gilbey SG, Watkins PJ. Perineurial calcification. Neuropathol Appl Neurobiol. 1988;14(2):105–23.
35. Falk RH, Comenzo RL, Skinner M. The systemic amyloidoses. N Engl J Med. 1997;337(13):898–909.
36. Klein CJ, Vrana JA, Theis JD, Dyck PJ, Dyck PJ, Spinner RJ, et al. Mass spectrometric-based proteomic analysis of amyloid neuropathy type in nerve tissue. Arch Neurol. 2011;68(2):195–9.
37. Peter J, Dyck PJBD, Engelstad J. “Pathologic Alterations of Nerves”. Peripheral neuropathy. 4th ed: W.B. Saunders;Philadelphia, Pennsylvania. 2005.
38. Nukada H, Dyck PJ. Acute ischemia causes axonal stasis, swelling, attenuation, and secondary demyelination. Ann Neurol. 1987;22(3):311–8.
39. Berini SE, Spinner RJ, Jentoft ME, Engelstad JK, Staff NP, Suanprasert N, et al. Chronic meralgia paresthetica and neurectomy: a clinical pathologic study. Neurology. 2014;82(17):1551–5.

40. Uceyler N, Necula G, Wagemann E, Toyka KV, Sommer C. Endoneurial edema in sural nerve may indicate recent onset inflammatory neuropathy. Muscle Nerve. 2016;53(5):705–10.
41. Hanyu N, Ikeda S, Nakadai A, Yanagisawa N, Powell HC. Peripheral nerve pathological findings in familial amyloid polyneuropathy: a correlative study of proximal sciatic nerve and sural nerve lesions. Ann Neurol. 1989;25(4):340–50.
42. Myers RR, Powell HC, Shapiro HM, Costello ML, Lampert PW. Changes in endoneurial fluid pressure, permeability, and peripheral nerve ultrastructure in experimental lead neuropathy. Ann Neurol. 1980;8(4):392–401.
43. Koike H, Iijima M, Sugiura M, Mori K, Hattori N, Ito H, et al. Alcoholic neuropathy is clinicopathologically distinct from thiamine-deficiency neuropathy. Ann Neurol. 2003;54(1):19–29.
44. Vital C, Vital A, Deminiere C, Julien J, Lagueny A, Steck AJ. Myelin modifications in 8 cases of peripheral neuropathy with Waldenstrom's macroglobulinemia and anti-MAG activity. Ultrastruct Pathol. 1997;21(6):509–16.
45. Vital C, Gherardi R, Vital A, Kopp N, Pellissier JF, Soubrier M, et al. Uncompacted myelin lamellae in polyneuropathy, organomegaly, endocrinopathy, M-protein and skin changes syndrome. Ultrastructural study of peripheral nerve biopsy from 22 patients. Acta Neuropathol. 1994;87(3):302–7.
46. Ohnishi A, Hirano A. Uncompacted myelin lamellae in dysglobulinemic neuropathy. J Neurol Sci. 1981;51(1):131–40.
47. Vital C, Brechenmacher C, Reiffers J, Lagueny A, Massonnat R, Julien J, et al. Uncompacted myelin lamellae in two cases of peripheral neuropathy. Acta Neuropathol. 1983;60(3–4):252–6.
48. Yoshikawa H, Dyck PJ. Uncompacted inner myelin lamellae in inherited tendency to pressure palsy. J Neuropathol Exp Neurol. 1991;50(5):649–57.
49. Vital C, Vital A, Bouillot S, Favereaux A, Lagueny A, Ferrer X, et al. Uncompacted myelin lamellae in peripheral nerve biopsy. Ultrastruct Pathol. 2003;27(1):1–5.
50. Busard HL, Gabreels-Festen AA, van ‘t Hof MA, Renier WO, Gabreels FJ. Polyglucosan bodies in sural nerve biopsies. Acta Neuropathol. 1990;80(5):554–7.
51. Bergouignan FX, Vital C. Occurrence of Renaut’s bodies in a peripheral nerve. Arch Pathol Lab Med. 1984;108(4):330–3.
52. Jefferson D, Neary D, Eames RA. Renaut body distribution at sites of human peripheral nerve entrapment. J Neurol Sci. 1981;49(1):19–29.
53. Luse SA. Electron microscopic studies of brain tumors. Neurology. 1960;10:881–905.
54. Tohgi H, Tabuchi M, Tomonaga M, Izumiyama N. Spindle-shaped, cross-banded structures in human peripheral nerves. Acta Neuropathol. 1977;40(1):51–4.
55. Lehmann J. Fibrous long-spacing collagen in the perineurium of human sural nerve. Clin Neuropathol. 1983;2(3):134–7.
56. Deprez M, de Groote CC, Gollogly L, Reznik M, Martin JJ. Clinical and neuropathological parameters affecting the diagnostic yield of nerve biopsy. Neuromuscul Disord NMD. 2000;10(2):92–8.